

# SHALLOW SEISMIC AND GEOTECHNICAL SITE SURVEYS AT THE TURKISH NATIONAL GRID FOR STRONG-MOTION SEISMOGRAPH STATIONS

O. Yilmaz<sup>1</sup>, E. Savaskan<sup>2</sup>, S. Bakir<sup>3</sup>, T. Yilmaz<sup>3</sup>, M. Eser<sup>1</sup>, S. Akkar<sup>3</sup>,  
B. Tuzel<sup>4</sup>, Y. Iravul<sup>4</sup>, O. Ozmen<sup>4</sup>, Z. Denizlioglu<sup>4</sup>, A. Alkan<sup>4</sup>, and M. Gurbuz<sup>4</sup>

<sup>1</sup> *Anatolian Geophysical, Istanbul, Turkey;* <sup>2</sup> *Bilgi2000 Soil Investigations, Istanbul, Turkey;*

<sup>3</sup> *Department of Civil Engineering, Middle East Technical University, Ankara, Turkey;*

<sup>4</sup> *Earthquake Research Center, Ministry of Reconstruction, Ankara, Turkey*

*E-mail: oz@anatoliangeo.com*

## ABSTRACT

We conducted shallow seismic site survey at 161 strong-motion stations of the national grid in order to estimate P- and S-wave velocities down to a depth of 30 m. At each station site, we also drilled a geotechnical borehole down to 30-m depth. The P- and S-wave velocities were then correlated with geotechnical borehole data. The ultimate objective is to use shallow seismic velocities and geotechnical soil profiles to correct recorded seismograms for the local site effects, and determine geotechnical earthquake engineering parameters, including wave attenuation, site response spectrum, *TA-TB* periods, change of maximum acceleration with depth, soil amplification, and susceptibility to liquefaction. An integrated data acquisition system that includes an accelerated impact source with a 50-kg weight, a 48-channel receiver cable with 2-m geophone interval and 4.5-Hz vertical geophones, and two 24-channel, 24-bit Geode recording units was used to acquire the shallow seismic data. We acquired three 48-channel seismic records at each of the station sites using the common-spread recording geometry. By applying nonlinear travelttime tomography to the first-arrival times picked from the shot records, we estimated a near-surface P-wave velocity-depth model for the site along the receiver spread. By applying Rayleigh-wave inversion to the surface waves isolated from the shot records, we estimated an S-wave velocity-depth profile for the site. In the borehole at each station site, we performed standart penetration tests (SPT) at 1.5-m depth interval, determined core recovery and rock quality, measured the ground-water level. We then conducted geotechnical laboratory measurements and determined the soil profile for each station site. All of the field data and the results of our investigations from the shallow seismic and geotechnical site surveys will eventually be made available via a centralized data base on the internet to scientists and engineers for future investigations in earthquake engineering. Specifically, the reported results from the seismic and geotechnical investigations will be used to determine geotechnical earthquake engineering parameters for each station site, including site-dependent response spectrum, short- and long-corner periods of design spectrum, change of maximum ground acceleration with depth, soil amplification, and investigation of susceptibility to liquefaction. The reported results will also be of great use in the derivation of ground-motion prediction equations that consider the shear-wave velocity dependent site influence.

**KEYWORDS:** shallow seismic, geotechnical site investigations, Rayleigh-wave inversion

## 1. SEISMIC DATA ACQUISITION

Locations for the 161 strong-motion stations of the National Grid are shown on the map of Turkey in Figure 1.

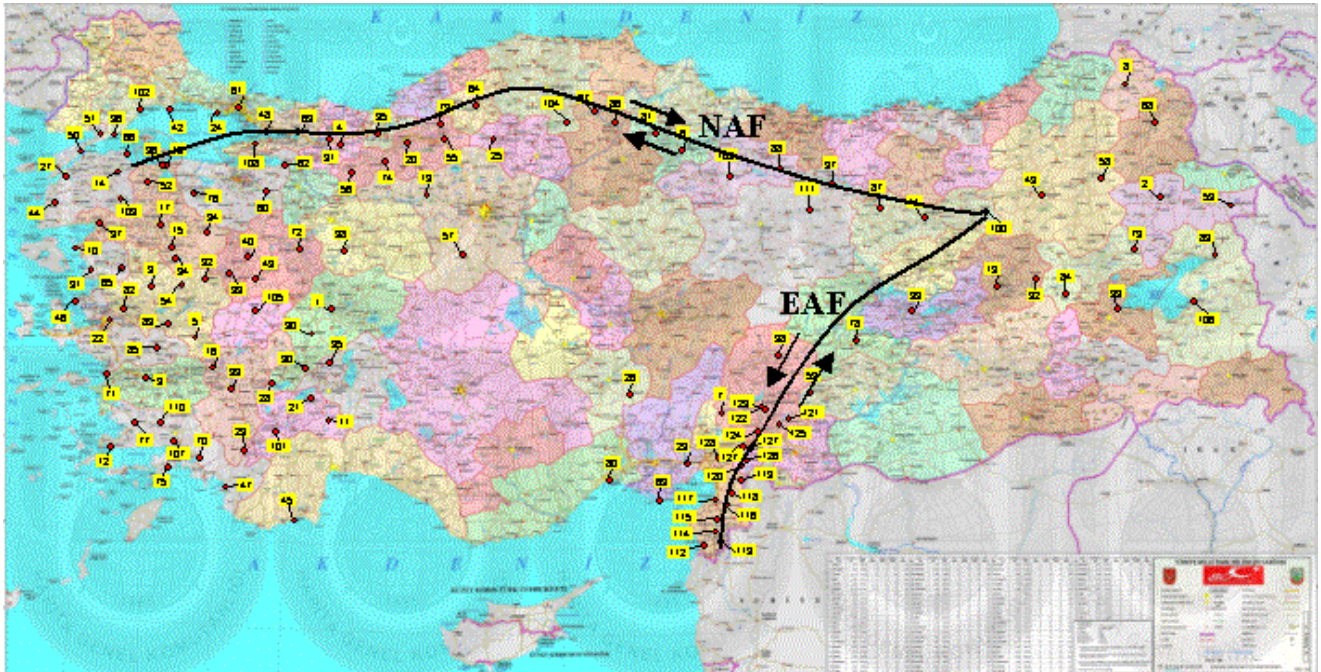


Figure 1. Location map for the Turkish National Grid for Strong-Motion Seismograph Stations. There are total of 161 seismograph stations. In the case of a few closely situated stations, all of them are represented by one dot. Note that the seismograph stations are located along the North Anatolian (NAF) and East Anatolian (EAF) strike-slip faults, and the Aegean and Marmara regions.

An integrated system that includes the source, cable and geophones has been designed and built for the seismic field work. The system components are listed in Table 1 and the data acquisition parameters are listed in Table 2.

Table 1. Components of the seismic recording system.

1	An impact source system that comprises a 50-kg weight with electromechanical acceleration and radio-controlled trigger
2	A 48-channel receiver cable with 2-m geophone interval and 96 4.5-Hz vertical geophones (a principal set of 48 units and a spare set of 48 units)
3	Two 24-channel Geode recording units
4	VW Volt vehicle, power inverter, four walkie-talkies, and one hand-held GPS unit

Table 2. Seismic acquisition parameters.

Receiver interval	2 m
Number of geophones in the spread	48
Geophone type	4.5 Hz, vertical
Spread length	94 m
Number of shots per spread	3
Shot points	2 m to the left of number 1 geophone, center of the spread in the middle of number 24 and 25 geophones, and 2 m to the right of number 48 geophone
Source type	50-kg accelerated weight
Sampling rate	1 ms
Trace length	2 s
Recording format	SEG2

The SEG2 format, which is standard in engineering seismology, was used to record the data. The field work at each station site was conducted as described below:

- (1) A custom-designed 94-m receiver cable with 48 4.5-Hz vertical geophones was laid out such that the center of the spread is as close as possible to the seismograph station, in a direction such that elevation differences between the geophone locations are negligibly small, and wherever possible on soil surface, if unavoidable, on asphalt or concrete surface. Geophones were planted firmly in soil, or into the asphalt or concrete using a hand-held drill.
- (2) An accelerated electromechanical impact source with 50-kg weight was positioned 2 m to the left of number 1 geophone on the line traverse of the spread. We preferred using a powerful and safely operated impact source in lieu of an explosive source, for most of the seismograph stations are located in towns inside or at the vicinity of buildings.
- (3) By the accelerated impact onto the ground surface, we acquired the first 48-channel seismic record.
- (4) While keeping the receiver spread, the impact source was positioned between number 24 and 25 geophones at the center of the spread, again on the line traverse of the spread as much as possible.
- (5) By the accelerated impact onto the ground surface, we acquired the second 48-channel seismic record.
- (6) Again, with the same receiver spread, the impact source was positioned 2 m to the right of number 48 geophone on the line traverse of the spread.
- (7) Finally, by the accelerated impact onto the ground surface, we acquired the third 48-channel seismic record.

We acquired three 48-channel seismic records as shown by the example in Figure 2 at each of the station sites using the common-spread recording geometry described above and the acquisition parameters listed in Table 2. When there was no sufficient traverse available for a 94-m receiver spread as close as possible to the seismograph station, the geophone interval was reduced to 1.5 or 1 m.

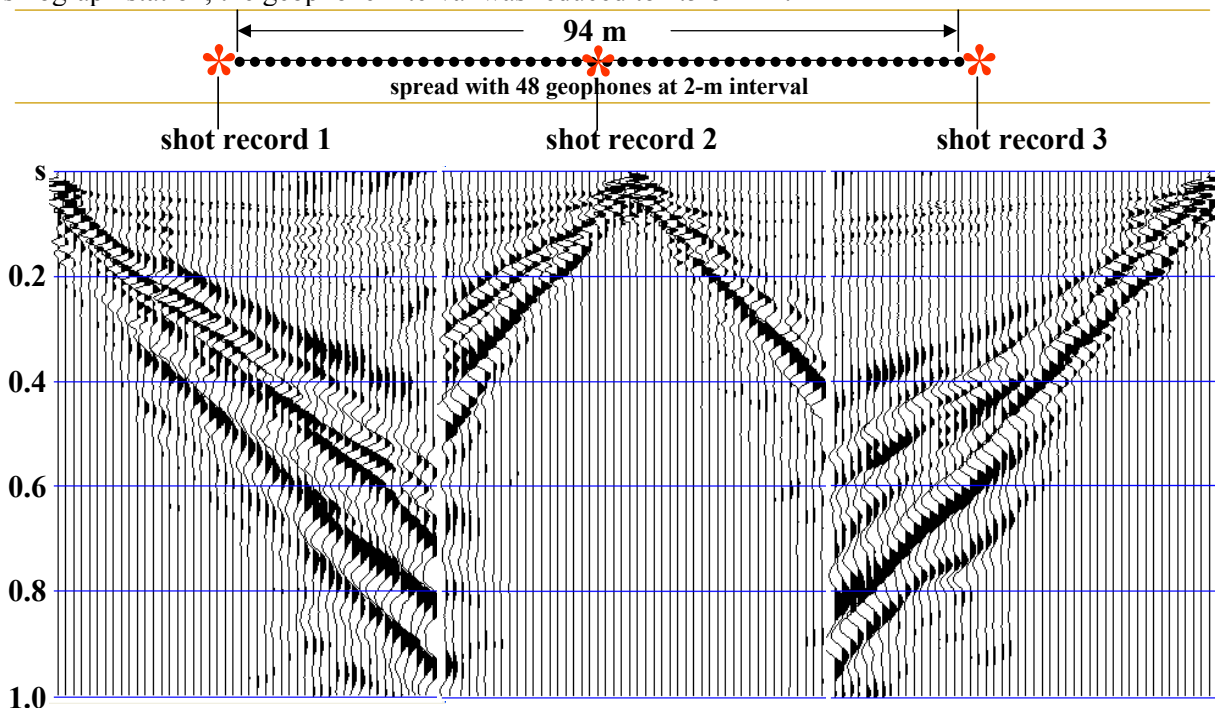


Figure 2. Example shot records at the site of station AI\_137\_DIN. These 48-channel records were acquired using a 50-kg accelerated impact source at the shot locations (indicated by the red asterisks) 2-m to the left, coincident with the center, and 2-m to the right of a 94-m spread with 48 4.5-Hz vertical geophones at 2-m intervals. The location of the geophone spread is indicated in the site sketch shown in Figure 3. The shot records predominantly contain dispersive Rayleigh wave energy.

## 2. SEISMIC DATA ANALYSIS

By applying a nonlinear traveltime tomography to the first-arrival times (Zhang and Toksöz, 1997) picked from the three shot records acquired at each station site, we estimated a near-surface P-wave velocity-depth model for the site along the receiver spread down to 30-m depth. By applying Rayleigh-wave inversion to the surface waves (Park et al., 1999; Xia et al., 1999) in the shot records acquired at each station, we estimated an S-wave velocity-depth profile for the site.

**Analysis of Refracted Waves.** First, an initial P-wave velocity-depth model is derived from the traveltimes picked from the field records (Figure 3). Then, this ‘initial’ model is perturbed iteratively by nonlinear traveltime tomography (Zhang and Toksöz, 1997) to estimate a ‘final’ P-wave velocity-depth model. At each iteration, first-arrival times are modeled and compared with the actual (picked) traveltimes (Figure 3). Iteration is stopped when the discrepancy between the modeled and actual traveltimes is reduced to an acceptable minimum. By computing the lateral average of the ‘final’ model, a P-wave velocity-depth profile for the station site is computed.

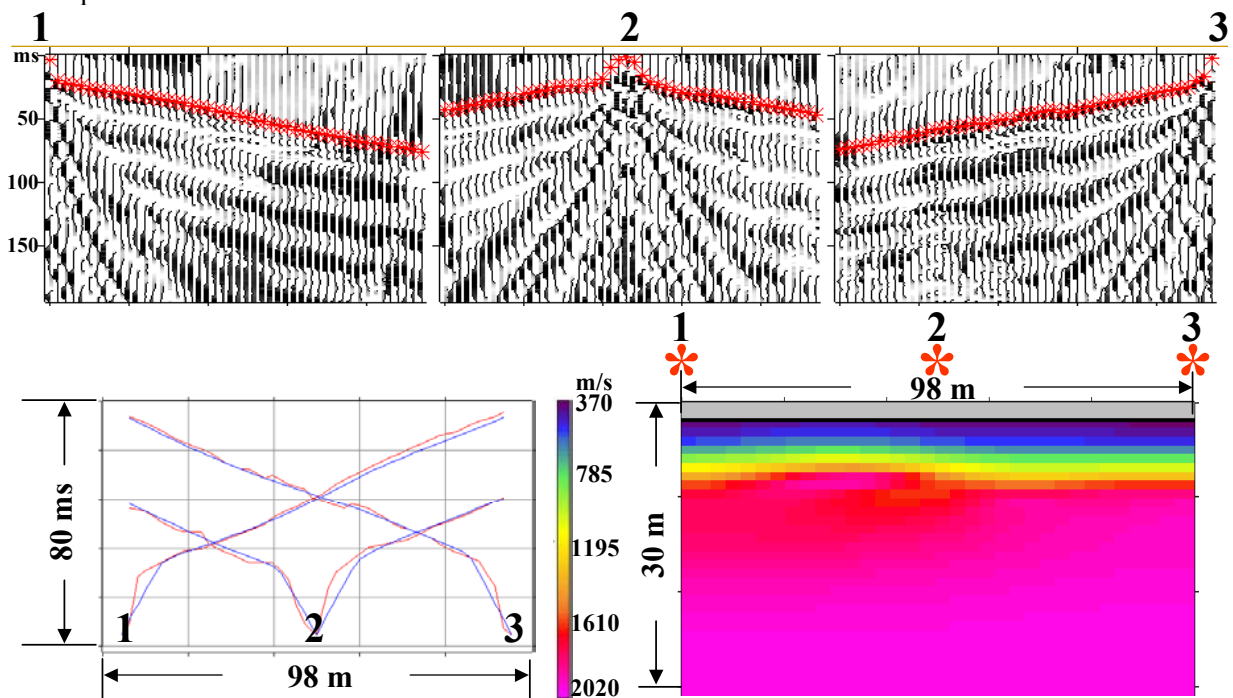


Figure 3. First-arrival times picked from the shot records acquired at the site of station AI\_137\_DIN (indicated by the red asterisks at the top) and the corresponding traveltime curves along the spread (represented by the red curves in the traveltime-distance graph at the bottom left). A P-wave velocity-depth model (bottom right) along the receiver spread was derived by iterative nonlinear tomography applied to the first-arrival times. By computing the lateral average of this model, a P-wave velocity-depth profile for each station site was computed with the numerical values listed in Table 1. The numbered asterisks denote the shot locations.

**Analysis of Surface Waves.** The velocity estimation from surface waves represents a lateral average over the receiver spread length in contrast with the velocity estimation from borehole seismic measurements which are influenced by localized lithologic anomalies and borehole conditions. In the analysis of surface waves, we used one of the off-end shot records at each station site with the most pronounced dispersive surface-wave pattern, which was first isolated from the refracted and reflected waves by inside and outside mute, then filtered using a 2,4-36,48-Hz passband to remove low- and high-frequency noise (Figure 4). Next, we performed plane-wave decomposition to transform the data from offset-time to phase-velocity versus frequency domain (Park et al.,

1999; Xia et al., 1999). A dispersion curve associated with the fundamental mode of Rayleigh-type surface waves was then picked in the transform domain (Figure 5) and inverted to estimate the S-wave velocity as a function of depth (Figure 4). In this procedure, initial depth-profiles for P- and S-wave velocities are iteratively perturbed until a final S-wave velocity-depth profile is estimated. At each iteration, modeled dispersion values and the picked (actual) dispersion values are compared (Figure 4). Iteration is stopped when the discrepancy between the modeled and actual dispersion values is reduced to an acceptable minimum.

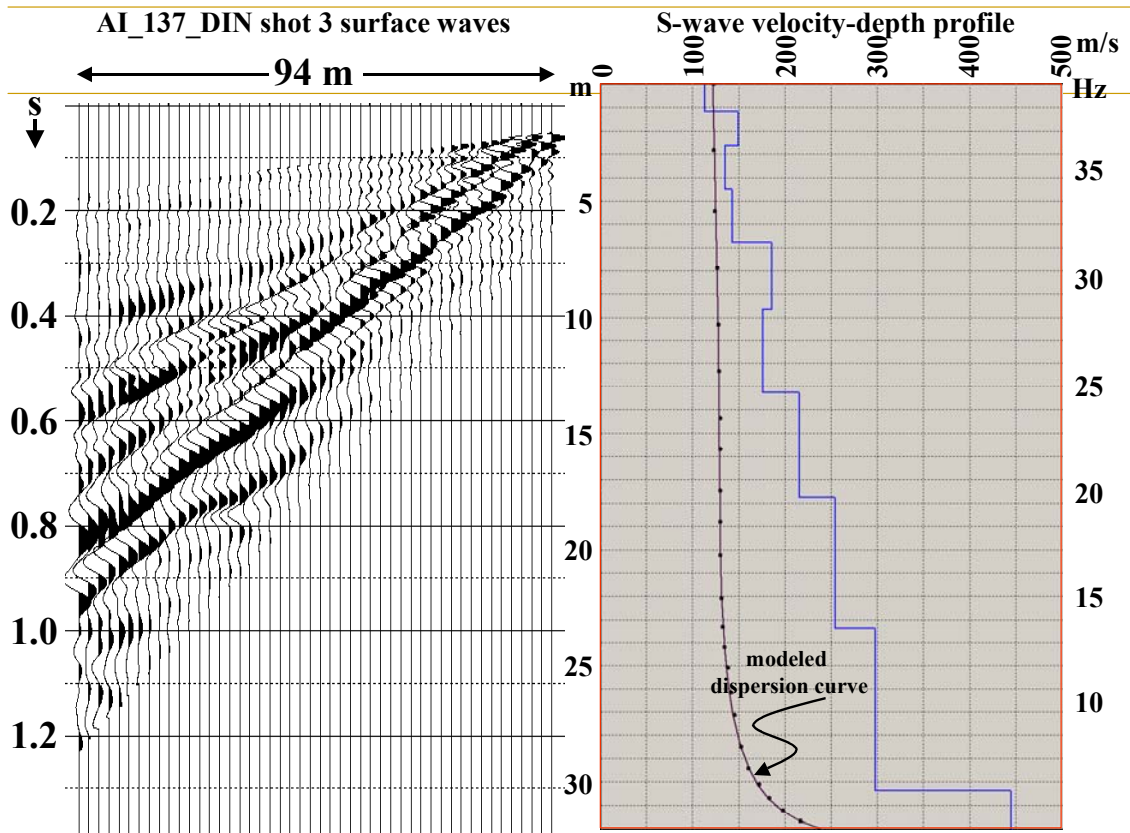


Figure 4. Left: one of the off-end shot records at the site of station AI\_137\_DIN after the isolation of surface waves and applying a frequency filter with 2,4-36,48-Hz passband to remove low- and high-frequency noise. Right: the S-wave velocity-depth profile (blue curve) and the modeled dispersion curve (black curve). The vertical axis in depth is associated with the S-wave velocity and the vertical axis in frequency is associated with the dispersion curve as in Figure 5. The S-wave velocity-depth profile was estimated by inversion of the dispersion curve for the Rayleigh-wave fundamental mode shown in Figure 5. The numerical values of the S-wave velocity-depth profile shown here are listed in Table 5.

Important aspects of surface-wave inversion are noted below.

- (1) From the dispersion curve, maximum depth to which the S-wave velocity can be estimated with sufficient accuracy is equal to  $(1/2) * (\text{maximum picked phase velocity} / \text{corresponding minimum frequency})$  (Rix and Leipski, 1991; Park et al., 1999).
- (2) Surface waves propagate as plane waves when the distance between the shot point and the nearest geophone (minimum offset) is greater than half the maximum wavelength (Stokoe et al., 1994). Additionally, maximum depth of penetration for surface waves is roughly equal to the maximum wavelength (Richart et al., 1970).
- (3) Based on the characteristics of surface waves described above, minimum offset can be approximately set to the maximum depth to which the S-wave velocity can be estimated. Nevertheless, P-wave velocity

estimation requires a minimum offset equal to the receiver interval and a maximum offset approximately three times the maximum depth of interest (32 m).

- (4) In this project, the field recording geometry (Table 2) was designed to obtain P- and S-wave velocity-depth profiles for a depth interval of 0-32 m.
- (5) Also from the dispersion curve, minimum layer thickness that can be resolved with an accurate S-wave velocity estimate is equal to  $(1/2) * (\text{minimum picked phase velocity} / \text{corresponding maximum frequency})$ . As such, for most of the stations, the estimated S-wave velocity-depth profile has a resolution of 1-2 m layer thickness.

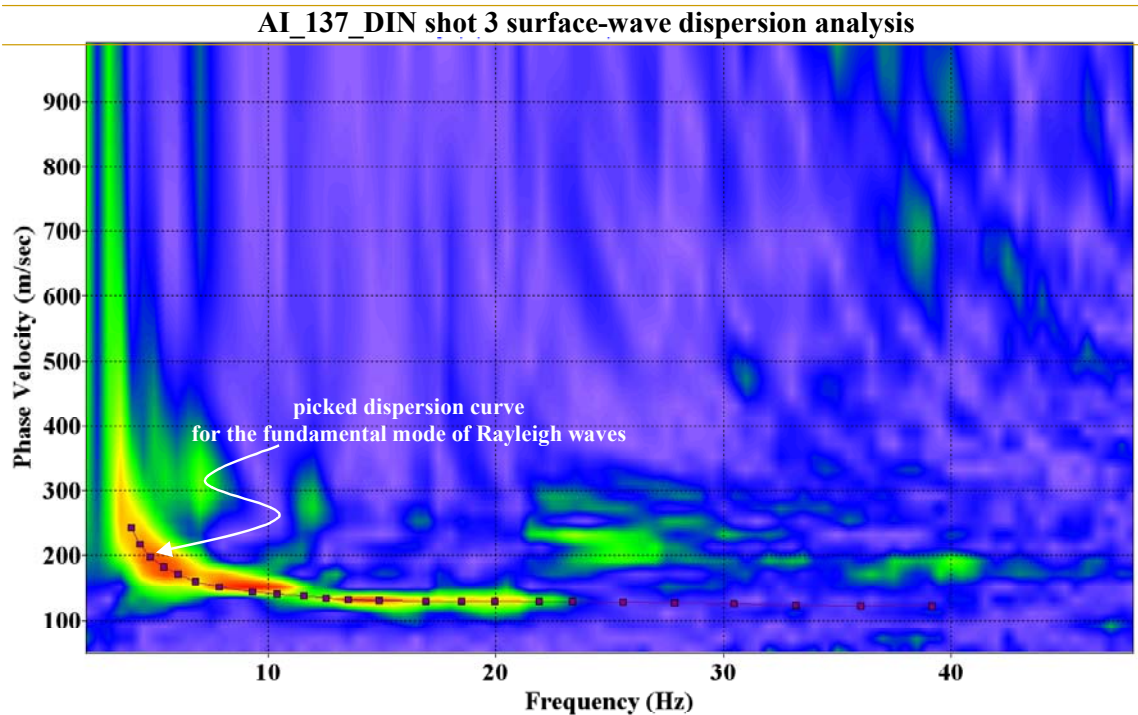


Figure 5. The dispersion spectrum of the surface waves in the shot record for the site of station AI\_137\_DIN shown in Figure 4, computed by plane-wave decomposition. In this figure, the vertical axis represents the phase velocity of Rayleigh waves. Note that each frequency component of the Rayleigh waves travels at a different speed --- thus the dispersive character of these waves within the soil column. The largest portion of the Rayleigh-wave energy often, but not always, is associated with the fundamental mode. For this mode, a dispersion curve that represents the change of phase velocity with frequency is picked as shown. Then, this dispersion curve is used in an inversion algorithm to estimate the S-wave velocity-depth profile for the soil column at the station site (Figure 4).

### 3. GEOTECHNICAL BORINGS AND LABORATORY TESTING

A geotechnical boring was carried out at each of the 153 sites for the National Grid for Strong-Motion Stations, using a rotary, truck-mounted drill rig. The borings were drilled with water flush, driving temporary casing to prevent caving of strata, where necessary. During advancement in soil, standard penetration tests (SPT) were carried out at 1.5 m intervals and disturbed samples were retrieved. In case cohesive soil strata of suitable consistency were encountered, undisturbed samples using Shelby tubes were also recovered. In rock, boreholes were advanced by continuous coring. In each borehole, the groundwater level was determined carefully. The flush water in the borehole was bailed out, completely if possible, then the depth to the phreatic level was measured after a few hours.

The planned boring length of 30 m was observed or revised based on the following criteria:

- (1) In case of encountering rock before the depth of 30 m was reached, the boring was stopped after a minimum coring length of 3 m in rock. However, if the rock were highly weathered or crushed, the advancement in rock was extended sufficiently to enable rock description. SPTs were performed in poor rock with little or no recovery.
- (2) In case the SPT values indicated soft or loose soil layers even at 30-m depth, the boring was extended to reach stiffer or denser strata below.
- (3) In case neither of the two criteria given above were satisfied, the boring was drilled to 30 m; only few exceptions being boreholes drilled in soils dominantly consisting of abrasive cobbles and boulders, where driving casing and preventing the hole from caving have not been possible.

The samples from boreholes were initially described and classified using a visual and manual procedure. The SPT  $N$  values were utilized for soil classification with respect to consistency (cohesive soils), and density (granular soils). The total core recovery (TCR) and rock quality designation (RQD) values of the rock cores were computed. All soil and rock samples also were studied as to their geologic origins and the borehole information was matched with the most recent geological map of Turkey at 1:500,000 scale published by the Turkish Mineral Research and Exploration Institute (MTA). A relevant segment of the same geologic map for each of the station sites, covering the accelerometer station and vicinity, was pasted on to the log, together with a brief description of geomorphologic features.

Generally, all disturbed and undisturbed soil samples were subjected to geotechnical laboratory testing. Tests on disturbed (SPT) samples include:

- (1) Sieve analysis on dominantly granular soils,
- (2) Sieve analysis, Atterberg limits and water content (where applicable) on mixed soils,
- (3) Atterberg limits and water content on almost purely cohesive soils.

On undisturbed samples of cohesive soils obtained with Shelby tubes, uniaxial compressive strength tests were carried out in addition to the classification tests. The soil classification was performed based on the Unified Soil Classification System (USCS). The soil class, uniaxial compressive strength, plasticity index, water content and percent passing the # 200 sieve are noted in the borehole logs.

#### **4. CONCLUSIONS**

Figure 6 shows correlation of seismic velocities with geotechnical borehole data for the example station site. In general, the S-wave velocities and the SPT  $N$  values in depth for most of the 161 station sites are remarkably consistent, especially, in alluvial soils. Any discrepancy between the S-wave velocities and the SPT  $N$  values can be attributed to the fact that the former represents the lateral average along the receiver spread while the latter is measured at the borehole location. Additionally, lateral heterogeneity, which can be roughly determined from the P-wave velocity-depth model along the receiver spread, and the borehole conditions must all be taken into consideration when comparing the S-wave velocities with the SPT  $N$  values.

Results from the seismic and geotechnical investigations will be used in the future to determine geotechnical earthquake engineering parameters for each station site, including site-dependent response spectrum, short- and long-corner periods of design spectrum, change of maximum ground acceleration with depth, soil amplification, and investigation of susceptibility to liquefaction. The reported results will also be of great use in the derivation of ground-motion prediction equations that consider the shear-wave velocity dependent site influence.

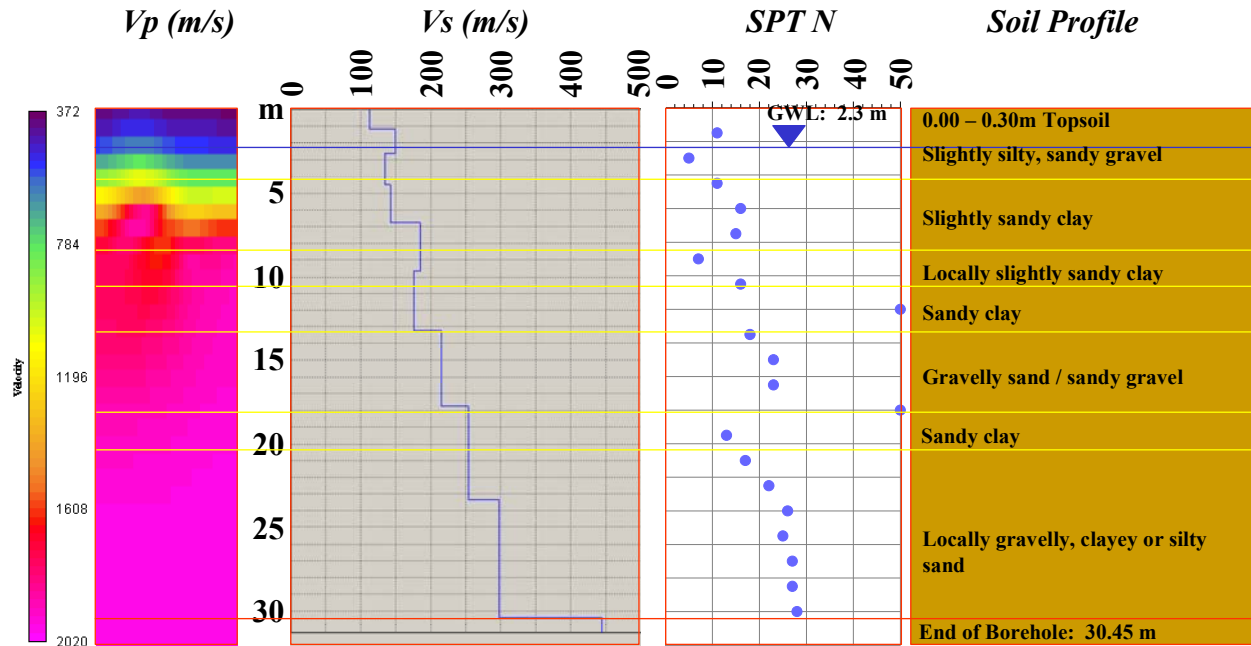


Figure 6. Integration of the results of seismic and geotechnical investigations at the site of station AI\_137\_DIN. From left to right: P-wave velocity-depth model (same as the model in Figure 3 squeezed laterally); the S-wave velocity-depth profile (same as the profile in Figure 4); uncorrected SPT  $N$  values measured at 1.5-m intervals; and the simplified form of the soil profile from the geotechnical borehole. The yellow horizontal lines define the layer boundaries within the soil column based on the geotechnical borehole log, the blue horizontal line represents the groundwater level (GWL), and the red horizontal line represents end of the borehole. GWL has not been observed over a long duration.

## ACKNOWLEDGEMENTS

This study was conducted as part of the project on “Compilation of Turkish Strong Ground Motion Database in Accordance with International Standarts” funded entirely by The Scientific and Technical Research Council of Turkey (TUBITAK) under Research Grant No. 105G016. We express our sincere gratitude for the support we received from TUBITAK during the two years of the duration of the project.

## REFERENCES

- Park, C. B., Miller, R. D., and Xia, J. (1999). Multichannel analysis of surface waves. *Geophysics*, **64**, 800-808.
- Richart, F. E., Hall, J. R., and Woods, R. D. (1970). *Vibrations of soil and foundations*, Prentice-Hall, Inc.
- Rix, G. J. and Leipski, E. A. (1991). Accuracy and resolution of surface-wave inversion, in *Bhatia, S. K. and Blaney, G. W., Eds., Recent advances in instrumentation, data acquisition and testing in soil dynamics*, Am. Soc. Civil Eng., 17-32.
- Stokoe, K. H., Wright, G. W., James, A. B., and Jose, M. R. (1994). Characterization of geotechnical sites by SASW method, in *Woods, R. D., Ed., Geophysical characterization of sites*, Oxford Publ.
- Xia, J., Miller, R. D., and Park, C. B. (1999). Estimation of near-surface shear-wave velocity by inversion of Rayleigh waves. *Geophysics*, **64**, 691-700.
- Zhang, J. and Toksöz, M. N. (1997). Joint refraction travelttime migration and tomography. *Proceedings of the Environmental and Engineering Geophysical Society*, Reno, Nevada, 901-910.